IMPROVED SHAPE DESCRIPTION USING RADON TRANSFORM AND APPLICATION IN PHYTOPLANKTON IDENTIFICATION

Kang Lin[1], Yang Chenhui[1*], Gao Yahui[2]

[1]School of Information Science and Technology, [2]School of Life Science,
Xiamen University, Xiamen
kanglinxm@gmail.com, chyang@xmu.edu.cn, gaoyh@jingxian.xmu.edu.cn

Abstract

An improved shape description using Radon transform is presented. As shown in the experiments for MPEG-7 shape database, the improved Radon composite features descriptor not only has rotation, scaling and translation invariance (RST), but also has better performance in image retrieval than Radon composite features (RCFs) and some well-known approaches such as Zernike moments and Gabor Filters. Phytoplankton is as one of important indication to the ocean ecosystem, the application of the improved Radon composite features in phytoplankton identification system is also shown in this paper.

Keywords: Radon transform; Invariance; Shape; Image retrieval; Phytoplankton identification

1. Introduction

Large collections of images are used in many areas now days, therefore, the effective ways of contend-based image searching are needed. Since visual information is hard to be described by words, other representations of images are useful. Shape is known as the most fundamental property of image, and it plays an important role in human recognition. Shape descriptors, can glancing be divided into two categories, contour-based and region-based descriptors [1]. Contour-based descriptors [7] use boundary information of shape, including spectral descriptors, shape signatures and global shape descriptors [2]. Region-based descriptors [10] use both boundary and all the pixels of the image information, including global and structural methods, depending on whether they separate shapes into sub parts or not [5].

Chen [4] proposed a shape description method named Radon composite features (RCFs) using Radon transform. It provided a novel feature-based invariant descriptor. The improved Radon composite feature (IRCFs) based on RCFs is obtained by more effective features, and it introduces the weight parameter for each feature. L1 Minkowski distance is used for computing distance measure between two shape images. Phytoplanktons are single-celled algae with silica exoskeletons which can take a variety of shapes [12]. It plays an important role as is one of indication to the ocean ecosystem. In Phytoplankton Identification System (PIS), shape is important information for phytoplanktons, and the IRCFs are used for image retrieval method as a part of the classifier.

This paper is structured as follows: Radon transform of image is explained in section 2 and the details of extraction and measurements of IRCFs are described in section 3. The effectiveness of IRCFs is shown with some experiment results under various test conditions in section 4. The simple applications of IRCFs in Phytoplankton Identification System show in section 5. And the paper concludes in section 6.

2. Radon transform

The Radon transform of an image is defined by [3]:

$$R_f(\rho,\theta)=\int_{-\infty}^{\infty}\int_{-\infty}^{\infty} f(x,y)\delta(x\cos\theta+y\sin\theta-\rho)dxdy, \quad (1)$$

where $\delta(\cdot)$ represents the Dirac Delta-function which ($\delta(f)=1$ only when $f=0$, elsewhere $\delta(f)=0$), $\theta\in[0,\pi)$, and $\rho\in(-\infty,\infty)$. $f(x,y)$ represents the image function.

For shape recognition field, it is of particular interest to consider the case that replaces the function $f(x,y)$ by:

$$f_D(x,y)=\begin{cases}1 \ if\,(x,y)\in D\\ 0 \ otherwise,\end{cases} \quad (2)$$

978-1-4244-4591-2/09/$25.00 ©2009 IEEE

where D is the domain of the binary shape image(Figure 1). Radon transform is linear, so geometric feature can be made obviously, and Figure 2 shows a simple device and its Radon transform.

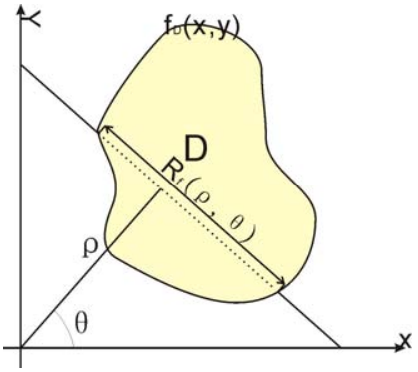

Figure 1. Radon transform of a shape image

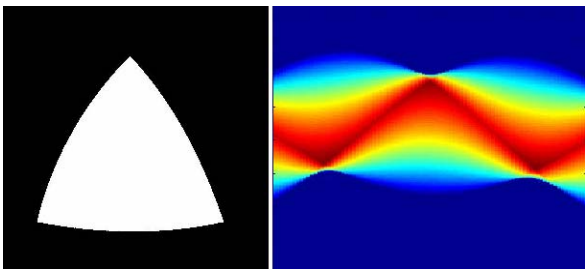

Figure 2. Shape image and its Radon transform

3. Extraction and similarity measurement of Radon composite features

In this section, we propose IRCFs which are invariant to rotation, translation and scaling. The overall binary image extraction process shows in Figure 3, and the similarity measurement is presented after the extraction process.

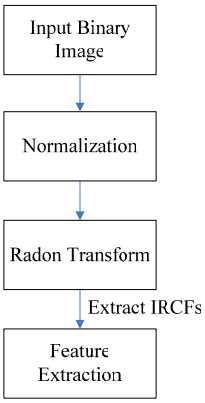

Figure 3. Extraction of IRCFs

3.1 Normalization

In our work, scaling invariance is obtained by normalizing [6] the image using the Cartesian moments prior to calculation of the IRCFs.

$$m_{0,0} = \iint f(x,y)dxdy, \tag{3}$$

The scale function $s(x_s, y_s)$ is defined by:

$$s(x_s, y_s): x_s = x \cdot \sqrt{\frac{\mu}{m_{0,0}}}, y_s = y \cdot \sqrt{\frac{\mu}{m_{0,0}}}, \tag{4}$$

where μ is a predetermined value.

3.2 Extraction Features

To a normalized binary image, we extract four features (3.2.1–3.2.4) for each angle $\theta_i (i = 1 \ldots n, n = 2^k, k \in Z)$, and then all features compose to a matrix of $n \times 4$ cells.

3.2.1 Feature I

Let $R_f(\theta_i)$ be Radon transform-signature, it obtains integral of whole image area. And its normalization form can be the IRCF feature.

$$R_f(\theta_i) = \int_{-\infty}^{\infty} R_f^2(\rho, \theta_i)d\rho, \tag{5}$$

$$F_{f,1}(\theta_i) = R_f(\theta_i) / \max(R_f(\theta_i)), \tag{6}$$

3.2.2 Feature II

Peak of binary image can describe the detail character of the shape. For each θ_i, the corresponding feature to describe the peak value of the shape image is:

$$F_{f,2}(\theta_i) = \frac{\sqrt{\pi}}{2\sqrt{\mu}} \max_{\rho} \{R_f(\rho, \theta_i)\}, \tag{7}$$

3.2.3 Feature III

The valid range of the image shape area along each θ_i can be described by $\rho_{\min}(\theta_i)$ and $\rho_{\max}(\theta_i)$, that is:

$$\rho_{\min}(\theta_i) = \arg\min_{\rho_j} \{R_f(\rho_j, \theta_i) > 0\}, \tag{8}$$

$$\rho_{\max}(\theta_i) = \arg\max_{\rho_j} \{R_f(\rho_j, \theta_i) > 0\}. \tag{9}$$

For an orthogonal direction pair θ_i and θ_j which satisfied:

$$\theta_j = \begin{cases} \theta_i - \frac{\pi}{2}, & if(\theta_i \in [\frac{\pi}{2}, \pi) \\ \theta_i + \frac{\pi}{2}, & if(\theta_i \in [0, \frac{\pi}{2}), \end{cases} \quad (10)$$

Along the θ_i, the degree of compactness of the Radon transformed signature can be measured by:

$$F_{f,3}(\theta_i) = \frac{\max\{R_f(\rho, \theta_i)\}}{\left\| \rho_{\max}(\theta_j) - \rho_{\min}(\theta_j) \right\|}. \quad (11)$$

$F_{f,3}(\theta_i)$ measures the degree of compactness of Radon translation signature along θ_i, it has much influence on the number of holes or fragment within the shape.

3.2.4 Feature Ⅳ

The mean square deviation of R_f for each direction shows the uniformity of distribution, and it can be normalized through (14).

$$\overline{R}_f(\theta_i) = \frac{\int_{-\infty}^{+\infty} R_f(\rho, \theta_i) d\rho}{\left\| \rho_{\max}(\theta_i) - \rho_{\min}(\theta_i) \right\|} \quad (12)$$

$$D_f(\theta_i) = \sqrt{\frac{\int_{-\infty}^{+\infty} (R_f(\rho, \theta_i) - \overline{R}_f(\theta_i))^2 d\rho}{\left\| \rho_{\max}(\theta_i) - \rho_{\min}(\theta_i) \right\|}} \quad (13)$$

$$F_{f,4}(\theta_i) = \frac{D_f(\theta_i)}{\max\{D_f(\theta_i)\}}. \quad (14)$$

3.2.5 IRCFs

Then, for a given binary shape image f, combine all four features above, the improved Radon composite features can be obtained:

$$IRCF_f(\theta_i) = (F_{f,1}(\theta_i), F_{f,2}(\theta_i), F_{f,3}(\theta_i), F_{f,4}(\theta_i)) \quad (15)$$

3.3 Similarity Measurement

All IRCFs features are translation invariant, and they are almost (some discrete error) scaling invariant after normalization. Given two binary shape images f_1 and f_2, the IRCFs of them are $F_{f_1,i}(\theta)$ and $F_{f2,i}(\theta)$. And L1 Minkowski distance is used to measure the similarity distance between two images, that is:

$$d(f_1, f_2, \Delta\theta) = \sum_{i=1}^{4} w_i \cdot d_{L1}(\left\| F_{f_1,i}(\theta) - F_{f_2,i}(\theta + \Delta\theta) \right\|) \quad (16)$$

$$d_{\min}(f_1, f_2) = \min_{\Delta\theta}(d(f_1, f_2, \Delta\theta)) \quad (17)$$

$$d_{\max}(f_1, f_2) = \max_{\Delta\theta}(d(f_1, f_2, \Delta\theta)) \quad (18)$$

$$d(f_1, f_2) = (1 + \frac{d_{\min}(f_1, f_2)}{d_{\max}(f_1, f_2)}) d_{\min}(f_1, f_2), \quad (19)$$

where w_i represent the weight of each IRCFs feature, and $d_{\min}(f_1, f_2)$ is rotation invariant. Of two similar shape images (except some very special shape, for example circle), the range between $d_{\min}(f_1, f_2)$ and $d_{\max}(f_1, f_2)$ is much different while comparing with two dissimilar shape images.

4. Experimental results

The number of scanning angle is significant, as it controls the precision of the descriptor. The parameters in our experiments are:

$$\mu = 4000, k = 5, w_1 = 0.2, w_2 = 0.4, w_3 = 0.2, w_4 = 0.2$$

This experiment involves the MPEG-7 Core Experiment (CE) shape-1 part B [7]. The database consists of 1,400 images with 20 images per category, some samples show in Figure 4. The retrieval rate for the query images are measured by counting the number of images from the same category which are found in the top n matches.

The retrieval rates on this database which used IRCF by compared with Zernike moment (ZM), RCF and Gabor Filters (GF) are shown in Table 1 and Figure 5.We can see that the IRCF achieves the best retrieval rate in most circs.

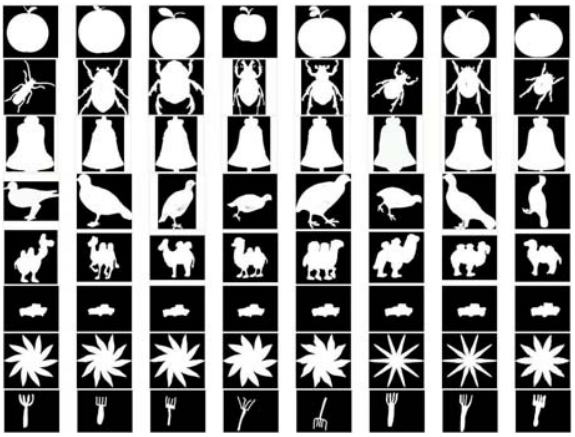

Figure 4. MPEG-7 CE-Shape-1 Part B samples

5. Application in PIS

Phytoplanktons are single-celled algae with silica exoskeletons which can take a variety of shapes. Phytoplanktons are widely used as ecosystem health

and evolution tracers. One of their most important characteristic is the fact that they vary their shape among different families and this can make possible its classification using pattern recognition techniques.

Table 1. Retrieval rate on MPEG-7 CE-shape-1 part B database

	Top n matches				
Methods	**n=1**	**5**	**10**	**15**	**20**
IRCF	100	81.72	**70.34**	**61.13**	**54.58**
RCF	100	**81.95**	69.16	60.15	52.61
GF	100	60.22	47.01	39.77	35.02
ZM	100	78.82	65.83	56.75	48.26

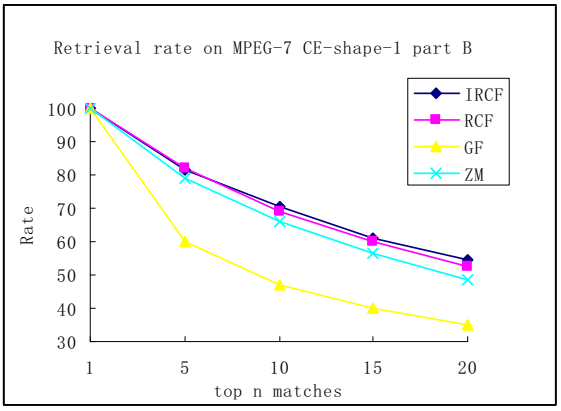

Figure 5. Retrieval rate on MPEG-7 CE-shape-1 part B database

There is an expert database which has more than 2000 pictures in PIS, so we can use the image retrieval techniques to classify the phytoplankton. Figure 6 shows some families of phytoplankton with different shapes.

Figure 6. Phytoplankton pictures of different families with different shapes (Pictures are originated from [14])

All images in the database are resized to 256x256 (using adaptive power law scaling methods to avoid distortion [9]) and each image is used successively as a query image and compared with all images in the database. Image should be processed before the IRCFs features extraction, Figure 7 shows the processed-picture in the database, and Figure 8 shows the result of top 5 matches using IRCFs in PIS.

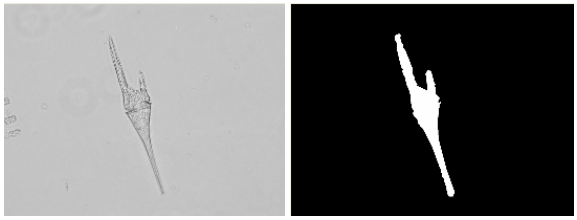

a b

Figure 7. Processing the picture in PIS database (a) Original image. (b) Processed shape image.

In PIS, the shape information is often not enough to distinguish all kinds of phytoplanktons. As the first-step classifier, shape features combined with texture features (such as gray level co-occurrence matrix [13] and roughness), are used in phytoplankton classification and have produced a good result.

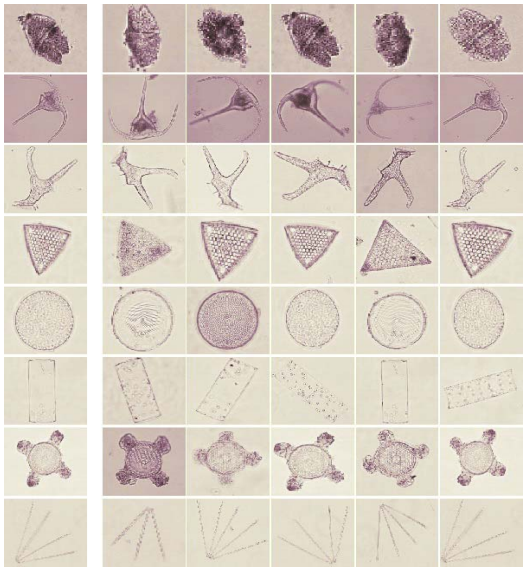

(a) (b)

Figure 8. Top 5 matches in PIS (a) Query image. (b) Top 5 matches in database (Gao et al, unpublished)

6. Conclusions

In this paper, we show that the improved Radon composite feature descriptor not only has rotation,

scaling and translation invariance, but also has better performance in image retrieval than RCF and some well-known approaches such as ZM and GF. It was very effective in retrieving an image from a large database, for example, the PIS, which has been mentioned in section 5.

Acknowledgments

Supported by the National Natural Science Foundation of China under contract No. 40627001.

*Corresponding author

Yang Chenhui, chyang@xmu.edu.cn, +86 136 06092025

References

[1] M. Bober. MPEG-7 visual shape descriptors. *IEEE Trans. Circuits Syst. Video Technol.*, vol. 11, no. 6, (Jun. 2001), 716-719.

[2] D. Zhang, and G. Lu. A comparative study on shape retrieval using Fourier descriptors with different shape signatures. In: Baiocchi, O.R., Syed, M.R. (Eds.), *Intelligent Multimedia, Computing and Communications Technologies and Applications of the Future*, Fargo, North Dakota, USA, (June. 2001), 1-9.

[3] V. F. Leavers, and J. F. Boyce, 1987. The Radon transform and its application to shape parameterization in machine vision. *Image Vision Comput.* vol. 5, no. 2, (May. 1987), 161-166. DOI= http://dx.doi.org/10.1016/0262-8856(87)90044-8

[4] Y.W. Chen, and Y.Q. Chen. Invariant Description and Retrieval of Planar Shapes Using Radon Composite Features. *IEEE Trans. Signal Processing*, vol. 56, no. 10, (Oct. 2008), 4762-4771.

[5] Y. Ebrahima, M. Ahmed, and W. Abdelsalam. Shape representation and description using the Hilbert curve. *Pattern Recognition Letters* vol. 30, (2009), 348-358.

[6] A. Khotanzad and Y. H. Hongs. Invariant image recognition by Zernike moments. *IEEE Trans. on Pattern Analysis and Machine Intelligence*, vol. 12, no. 5, (May. 1990), 489-497.

[7] L. J. Latecki, R. Lakamper, and U. Eckhardt. Shape descriptors for nonrigid shapes with a single closed contour. *Proc. IEEE Conf. Computer Vision and Pattern Recognition*, (2000), 424 – 429.

[8] G.A. Papakostas, Pattern classification by using improved wavelet Compressed Zernike Moments, *Appl. Math. Comput.* (2009), DOI = http://dx.doi.org/10.1016/j.amc.2009.02.029

[9] S. Tabbone, L. Wendling, and J.-P. Salmon. A new shape descriptor defined on the Radon transform. *Computer Vision and Image Understanding.* (November, 2005), 102, (2006), 42–51.

[10] M. E. Celebi, and Y. A. Aslandogan. A comparative study of three moment-based shape descriptors. *Proc. IEEE Int. Conf. Information Technology: Coding and Computing (ITCC)*, Las Vegas. vol.1, (Nov, 2005), 788–793.

[11] V. F. Leavers. Use of the Radon transform as a method of extracting information about shape in two dimensions. *Image Vis. Comput*. vol.10, no. 2, (1992), 99–107.

[12] R.E. Lokea, J.M.H. du Buf, M.M. Bayer, and D.G.Mannb. Diatom classification in ecological applications, *Pattern recognition*, vol. 37, (2004), 1283-1285.

[13] R.M. Haralick. Statistical and structural approaches to texture. *Proceedings of the IEEE*, vol. 67, no. 5, 1979, 786-804

[14] Z.D. Cheng, Y.H. Gao, and M. Dickman. Colour Plates of the Diatoms. *China Ocean Press*, Beijing (1996)